Nonlinear Wave Modeling and Dynamic Analysis of Internal Thermally Coupled Distillation Columns

Xinggao Liu, Yexiang Zhou, and Lin Cong
Dept. of Control Science and Engineering, State Key Laboratory of Industrial Control Technology, Zhejiang University, Hangzhou 310027, People's Republic of China

Jie Zhang
School of Chemical Engineering and Advanced Materials, University of Newcastle, Newcastle, Newcastle upon Tyne NE1 7RU, U.K.

DOI 10.1002/aic.12649
Published online May 2, 2011 in Wiley Online Library (wileyonlinelibrary.com).

Internal thermally coupled distillation column (ITCDIC) is a frontier in the energy saving distillation research. It is well known for the complex dynamics, which challenge the establishment of an excellent reduced model for further control strategy design greatly. In this article, a physical approach of the ITCDIC process based on nonlinear wave theory is explored, where it is first discovered that traditional wave theory in conventional distillation columns (CDIC) could not be directly applied in ITCDIC, due to: First, the internal thermal coupling results in mole flow rates varying evidently over each stage, which not only makes the wave modeling of the wave phenomenon in ITCDIC more difficult but also makes wave dynamics greatly different between ITCDIC and CDIC; Second, an interesting wave phenomenon of ITCDIC is discovered that waves located in the rectifying section and stripping section travel under opposite tendencies when the steady state is disturbed by the step change of thermal condition q*, one sharpens and the other is likely to spread synchronously, it means the movement of wave profiles in ITCDIC could not be simply described by shock wave velocity, which is usually used in wave modeling of CDIC; more seriously, shapes of the self-sharpening wave profiles in ITCDIC change obviously during the traveling processes, which further reveals that shape influence on wave velocity has to be considered in the wave modeling of ITCDIC. A rigorous wave velocity and a natural wave velocity are derived, respectively, based on which, the detailed analyses of traveling wave characteristics are carried out. A novel wave velocity, based on the profile trial function which has been well developed by Marquardt, is further derived to consider the obvious change of profile shape. And a completed nonlinear wave model of ITCDIC is thereby established by combining the proposed wave velocity with thermal coupling relations and material balance relations. The benzene-toluene system is illustrated as an example, where component concentration prediction and distinct dynamic characteristics are carried out in detail based on the proposed nonlinear wave models. The research results reveal the accuracy and validity of the proposed nonlinear wave model of ITCDIC.* © 2011 American Institute of Chemical Engineers *AIChE J*, 58: 1146–1156, 2012

Correspondence concerning this article should be addressed to X. Liu at liuxg@iipc.zju.edu.cn and J. Zhang at jie.zhang@newcastle.ac.uk.

Keywords: ITCDIC, wave modeling, variable flow rates, internal thermal coupling, nonlinear wave dynamics

Introduction

Distillation columns are the key equipments in the chemical industries, which are well known for their low energy efficiency. To reduce the energy consumption, many studies have been carried out and new columns have been proposed, among which distillation columns with heat integration technology have attracted much attention since 1970s when they were conceptually introduced by Mah et al.[1] Different configurations and pilot plant tests of these columns have been reported on the literature.[2–9] Based on the theoretical evaluations, an improved ideal configuration named internal thermally coupled distillation columns (ITCDIC) without either the reboiler or the condenser is further proved to have the maximum energy efficiency.[10,11] However, due to its higher degree of thermal coupling between the rectifying section and the stripping section, interactions are significantly intensified. Furthermore, dynamics of ITCDIC are more complicated with inverse responses and so on.[12,13] These distinct characteristics present a great challenge to the control strategy design for ITCDIC because it is difficult to develop an accurate reduced model to characterize the complex dynamic behaviors. On one hand, traditional linear approximating models are valid only in a small neighborhood of the nominal operating point and cannot capture the rich nonlinear behaviors of many processes. The use of linear model could not achieve the demand of tight control in ITCDIC. More seriously, some controllers based on linear model could not get a convergent output in the high-purity separation processes.[3,12,14] On the other hand, a mechanistic model[2,12] composed of invariably complex, coupled, nonlinear partial differential equations is difficult to be directly applied to control design in plant for their bad efficiency and complex constructions.[15,16] Hence, the establishment of a suitable reduced dynamic model of ITCDIC has been a bottle-neck problem.

Model reduction by physical approach is proved to be effective to overcome the problems above.[17] Early research on chromatography proposed a wave theory to describe systems with distributed parameters which often exhibits dynamic phenomena that resemble traveling waves, which can be represented by wave fronts, wave pulses, and wave train.[18] This theory has been successfully extended to ion exchangers, fix-bed adsorption, and CDIC. Using the temperature profiles, Luyben[19,20] pioneered a profile-position control strategy; Marquardt[21–24] developed a rigorous wave velocity formula and profile trial function on the basis of differential material balances with equilibrium relations, so detailed analysis of the propagation velocity is carried out, and a simple wave model for CDIC is established. Also, Marquardt[23,24] introduced a generic concept for wave models, and he did not concentrate on velocity formula alone but rather gave an even more thorough mathematical analysis of column dynamics; Amrhein considered developing of rigorous wave velocity in his Diploma thesis and Kienle[25] used this formula in ideal multicomponent distillation processes; Hwang[26–31] developed a systematic nonlinear wave theory for CDIC and successfully analyzed varied nonlinear dynamics like asymmetry behavior, response lags, disturbance pulse in binary distillation columns. From then on, wave traveling theory is widely used for low-order modeling of distillation columns. Balasubramhanya and Doyle[32,33] developed a low-order wave model for high-purity distillation columns with online updated profile parameters; Group led by Han[34–36] established concentration and temperature observers on the basis of wave velocity; Group led by Henson[37,38] developed a complete low-order dynamic wave model of cryogenic distillation columns. Profile estimators designed for wave models using temperature and component concentration were also systematically studied.[39,40] These models performed excellently in IMC, GMC, NMPC strategies. Wave theory is also extended to multicomponent distillation columns and reactive distillation columns.[25,41,42]. Hankins[43,44] developed a wave model with varied molar flow rates involving enthalpy and hold-up effects. The assumption of "constant pattern" waves still seems to hold true in CDIC. Wave theory tends to be a promising tool to characterize the complicated nonlinear dynamics in the separation processes.

However, since the construction of ITCDIC is very different from CDIC, the frame work of nonlinear wave propagation theory of CDIC could not be directly applied to reduced model development in the present work:

(1) Molar flow rates in ITCDIC change drastically over every stage, because the driving forces for the liquid flow rate in the rectifying section and the vapor flow rate in the stripping section are both provided by the heat transference between the two columns. Molar flow rates at the stages near the two ends of the columns are much smaller than those in the middle part.

(2) A distinct phenomenon is discovered in the present work: Wave profiles in the rectifying section and stripping section in ITCDIC travel with the opposite tendencies when the system responses to the change of thermal conditions q. For example, when the profile in the rectifying section tends to sharpen, the profile in the stripping section is likely to spread synchronously when q has a step change. Since the two profiles are related with each other by the thermally coupled relations, neither of them could be simply approximated to a shock layer, which is often used in CDIC.

(3) The shape of wave with self-sharpening tendency in ITCDIC changes more obviously than that in a CDIC. Though Marquardt and Amrhein,[22] Bian and Henson[38] have pointed out the influence of shape change, in the modeling of CDIC, the shape influence is usually ignored since it makes the wave velocity computation much difficult. However, according to the preceding presentation, shape influence on the movement of wave front has to be considered in ITCDIC.

Detailed analysis and modeling process is arranged as follows: a rigorous general wave velocity of ITCDIC with varied molar flow rates is developed in the "Analysis of Wave Traveling in ITCDIC" section, and error between the two profile position tracking curves by the rigorous wave velocity and shock wave velocity is studied, where the

influence of shape change on the movement of the profile is presented obviously. Interpretation of the errors is carried out in "Traveling tendency of the wave profile" section, where the distinct traveling tendencies in ITCDIC are analyzed on the basis of the natural wave velocity distribution, which reveals that wave travels much faster on the two ends of the column than the middle part. As a result, the shape of the profile changes obviously in both sharpening tendency and spreading tendency. Considering the difficulty of on-line computation of the rigorous general wave velocity of ITCDIC, a trial profile function is employed to develop a new wave velocity expression, based on which a complete nonlinear wave model of ITCDIC is established by combining with the thermally coupled relations. Taking benzene-toluene system as an illustration, predictions of the nonlinear wave model and a rigorous model are compared in the "Nonlinear Wave Model of ITDIC" section. Results show the high accuracy and high efficiency of the proposed nonlinear wave model. In "Analysis of dynamics of ITCDIC based on nonlinear wave model" section, the established nonlinear wave model is employed to explain two interesting dynamics, i.e., asymmetric behavior and inverse behavior in ITCDIC. Results are well agreed with the analysis based on the mechanistic model,[2] further revealing the capability of nonlinear wave model on the nonlinear dynamic behavior characterization.

Schematic and Principles of the Ideal ITCDIC

Figure 1 shows the schematic diagram of the ideal ITCDIC, where the rectifying section and the stripping section are separated into two columns. The manipulation of internal thermal coupling is accomplished through heat exchange between the two sections. To provide the necessary temperature driving force for the heat transfer from the rectifying section to the stripping section, the former is operated at a higher pressure than the latter. To adjust the pressure, a compressor and a throttling valve are installed between the two sections. Because of the internal thermal coupling, a certain amount of heat is transferred from the rectifying section to the stripping section and brings the downward reflux flow for the former and the upward vapor flow for the latter. As a result, a condenser and reboiler are not required and energy savings are realized.

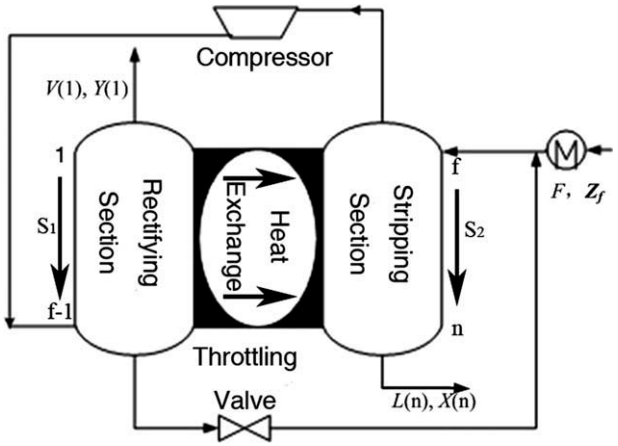

Figure 1. Schematic program of the Ideal ITCDIC.

Table 1. Component Balance Equations with Vapor-liquid Equilibrium Relationships

Component balances:

$$H\frac{dX_1}{dt} = V_2Y_2 - V_1Y_1 - L_1X_1 \qquad j = 1 \tag{1}$$

$$H\frac{dX_j}{dt} = V_{j+1}Y_{j+1} - V_jY_j + L_{j-1}X_{j-1} - L_jX_j \quad j = 2,\ldots,n \text{ and } j \neq f \tag{2}$$

$$H\frac{dX_f}{dt} = V_{f+1}Y_{f+1} - V_fY_f + L_{f-1}X_{f-1} - L_fX_f + FZ_f \qquad j = f \tag{3}$$

$$H\frac{dX_n}{dt} = -V_nY_n + L_{n-1}X_{n-1} - L_nX_n \qquad j = n \tag{4}$$

Vapor-liquid equilibrium relationships:

$$Y_j = \alpha X_j/[(\alpha - 1)X_j + 1] \qquad j = 1,2,\ldots,n \tag{5}$$

The distinct configuration of ITCDIC makes the manipulating variables different from a CDIC. Operating optimal analysis proves the feed thermal conditions q and the pressure of rectifying section p_r to be an efficient pair of operating variables.[12] And feed rate F, mole fraction of feed Z_f, heat transfer rate UA, pressure of stripping section p_s are main disturbances. When the stage numbered with the top as Stage 1 and the bottom as Stage n, and assuming the effect of holdup in the vapor phase is ignored, the basic component balance equations (light component) of the ideal ITCDIC are shown in Table 1.

Analysis of Wave Traveling in ITCDIC

The dynamic behavior of ITCDIC could be characterized by the propagation of wave profiles in the column sections. In this study, wave theory is extended to the dynamic analysis and reduced-order modeling of ITCDIC. Wave is defined as a monotonic variation of an independent variable (component concentration or temperature in CDIC), in ITCDIC, only considering component concentration, for the temperature is not monotonic change along the column. Each of the two sections of ITCDIC contains a wave profile, which is interacted with each other not only by the component balance on the feed tray but also by the coupled thermal relations between the two sections. The coupled thermal relations make the molar flow rates over each stage change dramatically. Hence, ITCDIC is more complex than a CDIC in which molar flow rates are usually regarded as constant.

In this section, the rigorous general wave velocity, shock wave velocity, and natural wave velocity of ITCDIC with varied molar flow rates are derived first. The errors of wave profile position tracked by the rigorous general wave velocity and shock wave velocity suggest the obvious shape influence on the movement of wave front evidently. A novel wave traveling analysis of the distinct wave traveling characteristics by natural wave velocity distribution interprets the cause-and-effect of the error sufficiently.

Generalized wave velocity of ITCDIC

Wave velocity is a key variable which could be derived based on the mass balance. The approximation formations of the staged balance relationships (1)–(4) are expressed as follows[23]:

$$h\frac{\partial X}{\partial t} = \frac{\partial (VY)}{\partial z} - \frac{\partial (LX)}{\partial z} \tag{6}$$

Table 2. Operation Conditions of ITCDIC

Operation conditions	Stage number n	Mole fraction of feed, Z_f	Feed thermal condition, q	Feed tray, f	Stage holdup, H/kmol
Value	40	0.5	0.501	21	1.5

Operation conditions	Heat transfer rate, UA/kW·K^{-1}	Feed rate, F/kmol·h^{-1}	Pressure of stripping section Ps/Mpa	Pressure of rectifying section Pr/Mpa
Value	9.803	100	0.1013	0.3387

where $z = \bar{z}/\Delta z$, and Δz is the height equivalent to a theoretical plate (HETP) and $\bar{z}$ is spatial coordinate. Then z becomes a dimensionless spatial coordinate belonging to [0 n], $h = H/\Delta z$.

Integrate (6) from the top to the feed tray, and the feed tray to the bottom respectively:

$$\int_0^{f-1} h\frac{\partial X}{\partial t}\,dz = \int_0^{f-1}\Big(\frac{\partial(VY)}{\partial z} - \frac{\partial(LX)}{\partial z}\Big)\,dz \tag{7}$$

$$\int_{f-1}^{n} h\frac{\partial X}{\partial t}\,dz = \int_{f-1}^{n}\Big(\frac{\partial(VY)}{\partial z} - \frac{\partial(LX)}{\partial z}\Big)\,dz \tag{8}$$

Wave velocity describes how fast the wave front travels. However, it is difficult to describe the exact position of the wave front, usually the sharpest point on the profile are chosen as a representation of the front. Denote wave front position (the sharpest point on the profile) in rectifying section and stripping section by S_1, S_2, respectively. Define $\varepsilon_1(t) = z - S_1(t)$ and $\varepsilon_2(t) = z - S_2(t)$ and transfer (7), (8) into wave traveling coordinate systems which is centered at the wave position ($\varepsilon_1 = 0$ and $\varepsilon_2 = 0$). After the algebraic transformations, the rigorous general wave velocity of ITCDIC is derived as follows:

$$\begin{aligned}\int_0^{f-1} h\frac{\partial X}{\partial t}\,dz &= \int_{-S_1}^{f-1-S_1} h\frac{\partial \tilde{X}}{\partial t}\Big(1+\frac{dS_1}{d\varepsilon_1}\Big)\,d\varepsilon_1 \\ &= \int_{-S_1}^{f-1-S_1} h\frac{\partial \tilde{X}}{\partial t}\,d\varepsilon_1 + h\frac{dS_1}{dt}(X_{f-1}-X_1)\end{aligned}$$

$$\begin{aligned}\int_0^{f-1} h\frac{\partial X}{\partial t}\,dz &= \int_0^{f-1}\Big(\frac{\partial(VY)}{\partial z} - \frac{\partial(LX)}{\partial z}\Big)\,dz \\ &= V_fY_f - V_1Y_1 - L_{f-1}X_{f-1}\end{aligned}$$

So,

$$\frac{dS_1}{dt} = \frac{V_fY_f - L_{f-1}X_{f-1} - V_1Y_1}{h(X_{f-1}-X_1)} - \frac{\int_{-S_1}^{f-1-S_1}\frac{\partial \tilde{X}}{\partial t}d\varepsilon_1}{X_{f-1}-X_1} \tag{9}$$

In the same way, there is:

$$\frac{dS_2}{dt} = \frac{-V_fY_f - L_nX_n + L_{f-1}X_{f-1} + FZ_f}{h(X_n - X_{f-1})} - \frac{\int_{f-1-S_2}^{n-S_2}\frac{\partial \tilde{X}}{\partial t}d\varepsilon_2}{X_n - X_{f-1}} \tag{10}$$

where $\tilde{X}$ denote the new liquid mole fraction of the rectifying section and stripping section in the moving wave coordinates respectively. From Eqs. 9 and 10, it is obvious that the wave velocity is driven by two effects: (1) the net flow of the light component to or from the column section $w_1(t)$, $w_2(t)$, i.e., the first part of the right side in Eqs. 9 and 10, respectively; (2) The influence of the shapes of the two concentration profiles $\phi_1(t)$, $\phi_2(t)$, i.e., the second part of the right side in Eqs. 9 and 10, respectively.

According to Antoine equation[2] with Raoult's law and Dalton's law, the heat between a pair of coupled stages is computed as follows:

$$\begin{aligned}Q_j = UA^*b\Big(&\frac{1}{a - ln\{p_r/[X_j + (1-X_j)/\alpha]\}} \\ &- \frac{1}{a - ln\{p_s/[X_{j+f-1} + (1-X_{j+f-1})/\alpha]\}}\Big), \\ &j = 1, 2, \ldots f-1\end{aligned} \tag{11}$$

And the vapor molar flow rates, liquid molar flow rates are computed as follows respectively:

$$V_1 = F(1-q) \tag{12}$$

$$L_n = Fq \tag{13}$$

$$L_{f-1} = \sum_{j=1}^{f-1}\frac{Q_j}{\lambda} \tag{14}$$

$$V_f = V_1 + L_{f-1} \tag{15}$$

Take a benzene-toluene system as an example. Operating conditions are given in Table 2. The system is disturbed by a 10% increase of feed rate F in ITCDIC. Figure 2 and Figure 3 show the two kinds of effects involving in the wave velocity formula.

Figure 2 visually shows the contribution of the two parts to wave velocity. The real lines denote dS_1/dt and dS_2/dt, the dashed lines denote $w_1(t)$ and $w_2(t)$, the lines with shadow area denote $\phi_1(t)$ and $\phi_2(t)$. From Figure 2, we can see clearly that dS_1/dt is negative and dS_2/dt is positive. The velocities of the two sections are opposite so the waves move in opposite direction. In another point of view, the increase of F increases the column's load and will make the two ends less pinched, so the waves will move in the direction of departing from the two ends and therefore in opposite direction. Take the rectifying section (left picture) as an illustrating section. Changing of $w_1(t)$ keeps in pace with the rigorous wave velocity (dS_1/dt), they have the same tendency, when the system comes to a new steady state, they both decrease to zero. In the wave theory of CDIC, $w_1(t)$ is usually used as an approximate wave velocity,

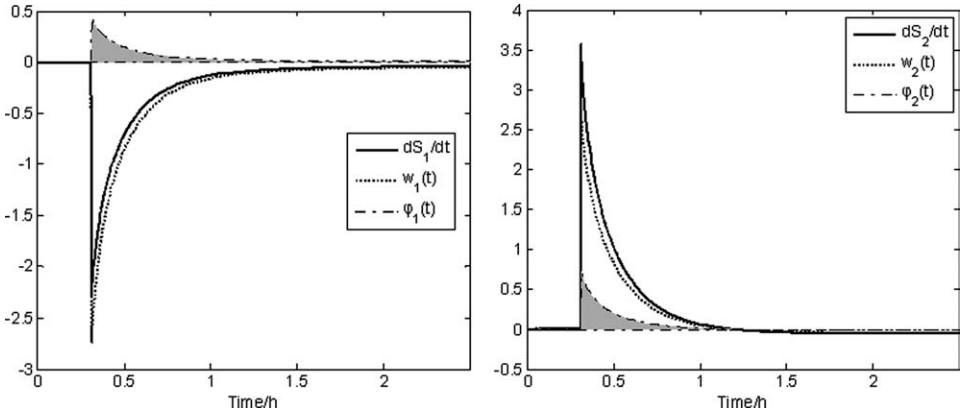

Figure 2. Transients of wave velocity components for +10% step disturbance of *F* in rectifying section (Left) and stripping section (Right).

which is named as shock wave velocity because $\phi_1(t)$ is much smaller than $w_1(t)$. Since $w_1(t)$ depends on mass balances with more simple formation than dS_1/dt, it could be conveniently applied to dynamic analysis and control strategy design to take the place of dS_1/dt. However to establish a nonlinear wave model with promising accuracy, the effect of $\phi_1(t)$ and $\phi_2(t)$ cannot be ignored. Especially at the very beginning, $\phi_1(t)$ makes great contribution to general wave velocity (almost a quarter of dS_1/dt). The situation in the stripping section is the same.

Figure 3 clearly presents the tracking error of the wave positions in ITCDIC by the general wave velocity and shock wave velocity. In the rectifying section, error between the real line and dashed line is equal to the integration of $\phi_1(t)$ with time (shadow area in Figure 2), when the system enters a new steady state, the absolute error increases to 0.11, about 23% of the total traveling distance of the wave position (0.48). In the stripping section, the absolute error increases to 0.1, about 20% of the traveling distance of the wave position (0.49).

The preceding analyses have revealed that shape changes have strong impact on wave velocity in ITCDIC, especially in the initial period when the system steady state is broken, though the effect gradually decreases to zero with the stabilizing of the system, the accumulated error in wave position change could not be negligible. A cause-effect analysis is carried out in the next section based on natural wave velocity distribution.

Traveling tendency of the wave profile

Wave velocity at different component concentrations (located at different stages) varies obviously in a high-purity ITCDIC, which makes the wave front either sharpen or spread during the traveling process. Traveling tendency mainly depends on two aspects: (1) original shape of the profile; (2) monotony of the natural wave velocity with respect to the mole fraction of liquid. First of all natural wave velocity at each stage is derived excluding the two ends and the feed tray as follows:

$$\left.\frac{dS}{dt}\right|_{X_j} = \frac{V_{j+1}Y_{j+1} - V_jY_j + L_{j-1}X_{j-1} - L_jX_j}{h(X_{j-1} - X_j)} \qquad j = 2, 3, \ldots, n-1 \ \text{and} \ j \neq f \quad (16)$$

Natural wave velocity of ITCDIC Eq. 16 is not only related with the equilibrium relation but also related with the varied molar flow rates (L, V). By changing the feed thermal condition q ($q = 1$ denotes saturated liquid, $q = 0$ denotes saturated vapor) of the ITCDIC, five steady wave profiles of

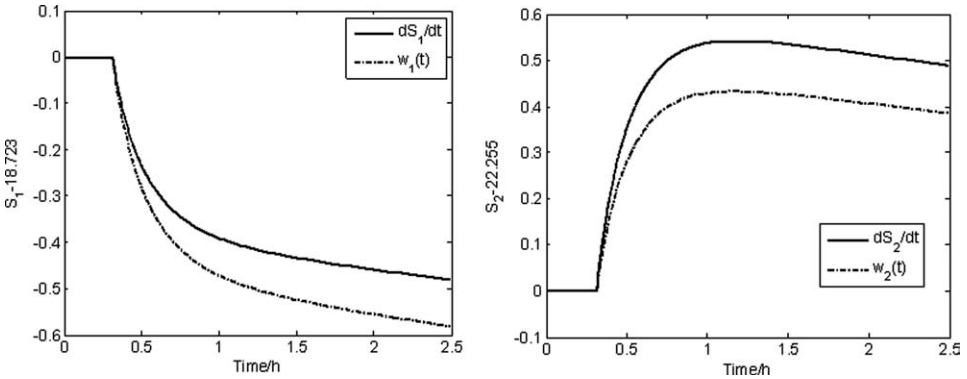

Figure 3. Traveling of wave front position for +10% step disturbance of *F* in rectifying section (Left) and stripping section (Right).

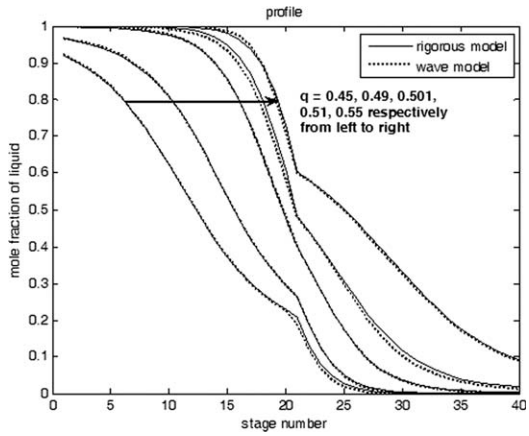

Figure 4. Profiles of mole fraction of liquid.

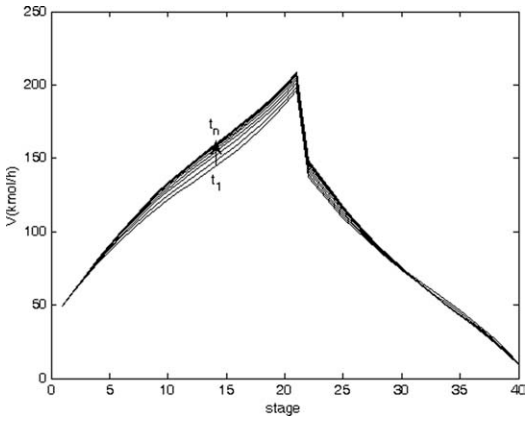

Figure 6. Vapor flow rate distribution when q is changed from 0.501 to 0.51.

mole fractions of liquid are derived as shown in Figure 4, and two travel processes of the profiles are studied.

Figure 5 shows the detailed natural wave velocity distributions at different time during the travel processes. Take rectifying section as shown in the left part as an illustration. Increasing the feed rate q from 0.501 to 0.51 at 0.3125 h, the natural wave velocities at different stage are recorded every 1.25 h from $t_1 = 2.5$ h as shown in the dashed lines. The system reaches a new steady state at t_n. Natural wave velocities at different times all decrease with the stage number (increase with the mole fraction). This monotonic character makes wave near the pinched end (top stage) keep on traveling faster than the other parts of the profile during the whole process. When the profile travels towards right as shown in Figure 4, the pinched end of the profile in the rectifying section tends to become more pinched, and the profile is likely to become a discontinued layer. Hence, this traveling process is defined as a self-sharpening wave. However, as shown in Figure 5, before $t_6 = 10$ h, natural wave velocity varies drastically at different stages which leads to obvious shape change. After t_6, natural wave velocity varies slightly over each stage so the profile could be approximated to a shock wave with constant-pattern. In this study, the period before t_6 is mentioned as transition period in the traveling process of a self-sharpening wave profile, during which, the effect on wave traveling speed from the shape should be taken into consideration. The vapor and liquid molar flows at different stages are also recorded every 1.25 h from $t_1 = 2.5$ h when q is changed to 0.51, which can be seen from Figures 6 and 7.

Natural wave velocity distributions of the rectifying section in the travel process by decreasing q from 0.501 to 0.49 as shown by the real line in the left part of Figure 5 have the opposite monotonic character of the natural velocity distribution shown by the dashed line. Contrast to the traveling direction of the preceding process, the profile travels downward, which makes the profile in the rectifying section spread to a less pinched one. And during the transition time (before $t_8 = 12.5$ h) the profile shape changes drastically, too. The vapor and liquid molar flows at different stages are recorded every 1.25 h from $t_1 = 2.5$ h when q is changed to 0.49, which can be seen from Figures 8 and 9.

Traveling tendency in the stripping section is much like the analysis presented above, as shown in Figure 4. An interesting phenomenon in ITCDIC is discovered for the first time that the travel tendencies in the stripping section and in the rectifying section are opposite to each other in response to the step change of the feed thermal conditions q as shown in Figure 5

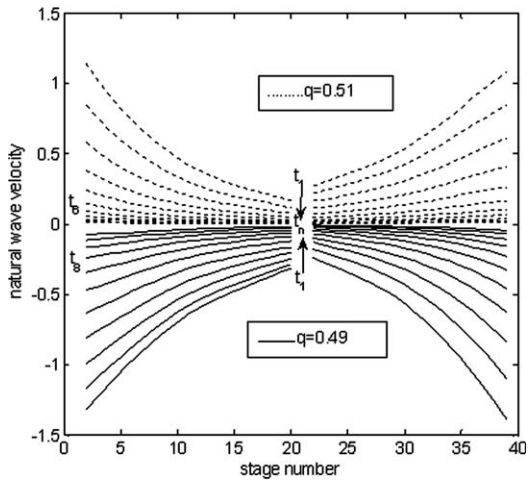

Figure 5. Natural wave velocity distribution.

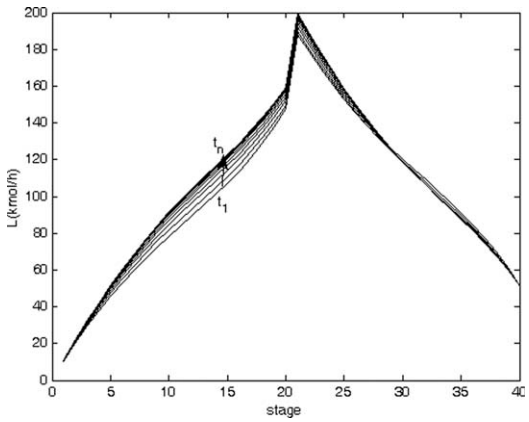

Figure 7. Liquid flow rate distribution when q is changed from 0.501 to 0.51.

obviously. The monotony tendencies of the natural wave velocity of the two sections are contrary. Hence, both self-sharpening wave and nonsharpening wave have to be considered simultaneously in the wave modeling process, which is much different from a conventional distillation column, in which usually the nonsharpening wave can be ignored.

The traveling tendency of wave profile in ITCDIC directly explains the cause of the error between profile positions tracked by the shock velocity and the rigorous general wave velocity. Analysis proves a fact that the error could not be eliminated for the reason that a long transition period exists before the self-sharpening wave becomes a shock one with constant pattern; furthermore, nonsharpening waves and self-sharpening waves co-exist in the dynamic process of ITCDIC. As a result, to characterize the dynamics of ITCDIC, tracking the shape change of the profile is requisite.

Nonlinear Wave Model of ITCDIC

Description of the profile

In the researches of many separation processes with distribution characteristics, a trial function is usually employed to describe the shape of the wave front. The stability and existence of the function has been proved in many literatures.[17,21,45] In ITCDIC, profiles in Figure 4 suggest two characteristics of the trial function: (1) asymptotic properties at the boundaries of the trial function; (2) exist only one inflection point in the definition field of the function. A trial function which has been successfully applied to high-purity CDIC[32,37–40] is introduced for ITCDIC as follows:

$$\hat{X}_j = X_{r\_\min} + \frac{X_{r\_\max} - X_{r\_\min}}{1 + \exp(-k_r(j - S_1))} \quad j = 1,2,\ldots,f-1 \tag{17}$$

$$\hat{X}_j = X_{s\_\min} + \frac{X_{s\_\max} - X_{s\_\min}}{1 + \exp(-k_s(j - S_2))} \quad j = f,f+1,\ldots,n \tag{18}$$

where $\hat{X}_j$ denotes the estimation of liquid mole fraction; $X_{r\_\min}$ and $X_{r\_\max}$ denote the asymptotic limits of the rectifying section when the profile extend to a infinite distance; $X_{s\_\min}$ and $X_{s\_\max}$ denote the asymptotic limits in the stripping section. $X_{r\_\max}$ and $X_{s\_\min}$ approximate to the liquid mole fraction at the top stage and the bottom stage respectively. k_r, k_s characterize the tangent of the inflection points S_1 and S_2 (k_r,,k_s do not equal the tangents). The inflection point S_1, S_2 are also the representations of the profile position in the rectifying section and stripping section, respectively.

Wave velocity based on the profile function

Based on the profile trial function, a new wave velocity combined with thermal coupled relations of ITCDIC could be derived. The relationships between wave velocity and the mass balance are established by the derivatives of profile Eqs. 17 and 18 as follows:

$$\frac{d\hat{X}_j}{dt} = \frac{(\frac{dk_r}{dt}(S_1 - j) + k_r\frac{dS_1}{dt})(X_{r\_\max} - \hat{X}_j)(\hat{X}_j - X_{r\_\min}) - \frac{dX_{r\_\max}}{dt}(\hat{X}_j - X_{r\_\min}) - \frac{dX_{r\_\min}}{dt}(X_{r\_\max} - \hat{X}_j)}{X_{r\_\min} - X_{r\_\max}} \quad j = 1,2,\ldots,f-1 \tag{19}$$

$$\frac{d\hat{X}_j}{dt} = \frac{(\frac{dk_s}{dt}(S_2 - j) + k_s\frac{dS_2}{dt})(X_{s\_\max} - \hat{X}_j)(\hat{X}_j - X_{s\_\min}) - \frac{dX_{s\_\max}}{dt}(\hat{X}_j - X_{s\_\min}) - \frac{dX_{s\_\min}}{dt}(X_{s\_\max} - \hat{X}_j)}{X_{s\_\min} - X_{s\_\max}} \quad j = f,f+1,\ldots,n \tag{20}$$

where $\frac{dS_1}{dt}$ and $\frac{dS_2}{dt}$ denote average movement of the entire profile in rectifying section and stripping section respectively.

Substitute $\frac{d\hat{X}_j}{dt}$ for $\frac{dX_j}{dt}$ in (1)–(4), after the algebraic transformations, the wave velocity are derived:

$$\frac{dS_1}{dt} = \frac{\frac{1}{H}(-V_1Y_1 + V_fY_f - L_{f-1}X_{f-1}) - \sum_{j=1}^{f-1}\frac{\frac{dX_{r\_\max}}{dt}(X_j - X_{r\_\min})}{X_{r\_\max} - X_{r\_\min}} - \sum_{j=1}^{f-1}\frac{\frac{dX_{r\_\min}}{dt}(X_{r\_\max} - X_j)}{X_{r\_\max} - X_{r\_\min}} + \sum_{j=1}^{f-1}\frac{(X_{r\_\max} - X_j)(X_j - X_{r\_\min})}{X_{r\_\max} - X_{r\_\min}}\frac{dk_r}{dt}(S_1 - j)}{-\sum_{j=1}^{f-1}\frac{k_r(X_{r\_\max} - X_j)(X_j - X_{r\_\min})}{X_{r\_\max} - X_{r\_\min}}} \tag{21}$$

$$\frac{dS_2}{dt} = \frac{\frac{1}{H}(-V_fY_f + L_{f-1}X_{f-1} + FZ_f - L_nX_n) - \sum_{j=f}^{n}\frac{\frac{dX_{s\_\max}}{dt}(X_j - X_{s\_\min})}{X_{s\_\max} - X_{s\_\min}} - \sum_{j=f}^{n}\frac{\frac{dX_{s\_\min}}{dt}(X_{s\_\max} - X_j)}{X_{s\_\max} - X_{s\_\min}} + \sum_{j=f}^{n}\frac{(X_{s\_\max} - X_j)(X_j - X_{s\_\min})}{X_{s\_\max} - X_{s\_\min}}\frac{dk_s}{dt}(S_2 - j)}{-\sum_{j=f}^{n}\frac{k_s(X_{s\_\max} - X_j)(X_j - X_{s\_\min})}{X_{s\_\max} - X_{s\_\min}}} \tag{22}$$

where molar flow rate L, V in (21) (22) are mainly decided by the accumulated heat transfer between the rectifying section and stripping section.

The profile function Eqs. 17, 18, the wave velocity Eqs. 21, 22, and the algebraic function Eqs. 11–15 construct the nonlinear wave model of ITCDIC.

Model test

Dynamics of the ITCDIC is mainly characterized by the traveling of the sharpest point on the profile. Liquid mole fractions of the stages near the sharpest points in the rectifying section and stripping section are the most important and need to be tracked efficiently. In this work, Benzene-toluene

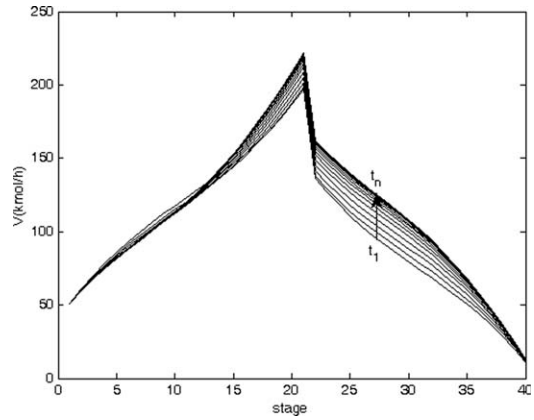

Figure 8. Vapor flow rate distribution when q is changed from 0.501 to 0.49.

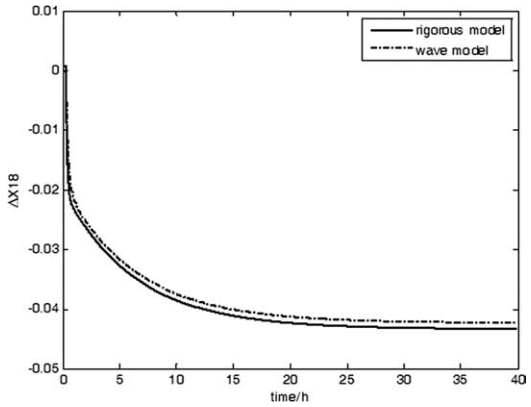

Figure 10. Comparison of liquid mole fraction on Stage 18.

system is taken as an illustration. The system with the operating conditions presented in Table 2 is disturbed by a +10% step change from the feed flow F at 0.3125 h. The tracking curves of the liquid mole fraction at Stage 18 and 23 by the wave model and a rigorous stage-by-stage model in Refs. 2 and 11 are presented in Figures 10 and 11.

Figure 10 shows that tracking deviations at Stage 18 at original steady state is about 7×10^{-4}. At 0.3125 h, the steady system is disturbed by the step change of feed rate F, and reaches a new steady state in 2.2 h. The average error between the two tracking curves is about -1.47×10^{-4}, compared with the deviation of the mole fraction from the original value (2.89×10^{-2}), the relative error is less than 0.5%.

Figure 11 shows the comparison of liquid mole fraction at Stage 23. Tracking error at original steady state is about -1.24×10^{-3}, average error during the travel process is about -1.36×10^{-4}.

The above comparison results strongly prove the efficiency of the proposed nonlinear wave model. Tracking error between the two models is small enough during the dynamic analysis and control strategy design.

Analysis of Dynamics of ITCDIC Based on Nonlinear Wave Model

Asymmetric behavior

Asymmetric behavior in high-purity distillation column has attracted much attention of researchers. Hwang[28] successfully employed traveling wave profile to explain this behavior in CDIC. In this work, a novel method by observing the wave velocity is carried out to analyze the asymmetric dynamics in ITCDIC.

In ITCDIC, responses of feed thermal condition q have the strongest asymmetric behaviors. So, the dynamics during the transient process caused by the change of q is studied as an illustration. The asymmetric behavior in ITCDIC refers to two kinds of distinct characteristics: (1) responses to positive and negative change are completely different in terms of stability time and deviations from the original state; (2) a transition departing from the balanced steady state (maximum separation state) is much faster than that returning to it. When $q = 0.501$, the illustrating benzene-toluene system is maintained at a balanced state.

Figure 12 shows the liquid mole fractions change over every stage. The peak points corresponding to the sharpest point on the concentration profiles presented in Figure 4 are visible representations of the profile positions.

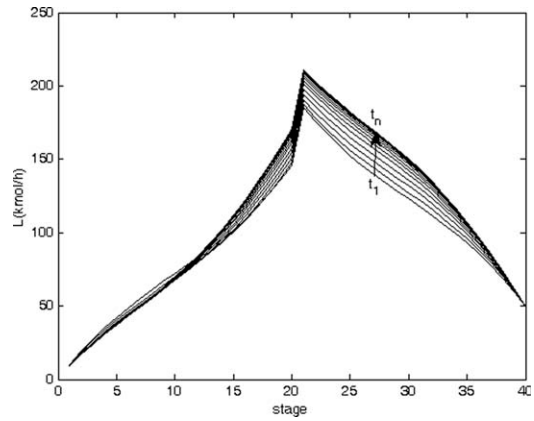

Figure 9. Liquid flow rate distribution when q is changed from 0.501 to 0.49

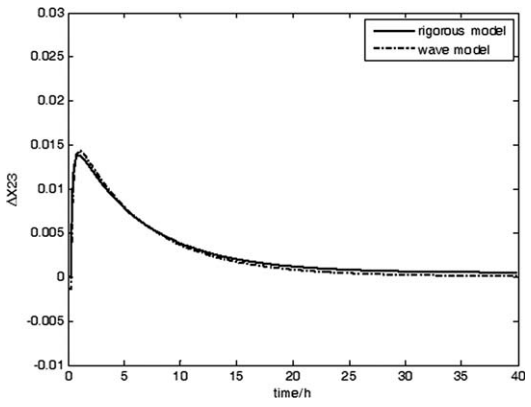

Figure 11. Comparison of liquid mole fraction on Stage 23.

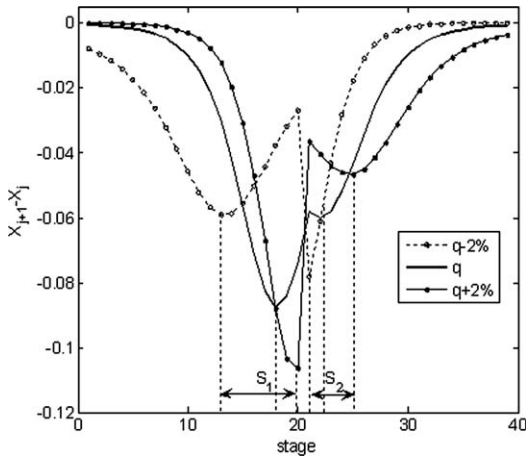

Figure 12. Profiles of concentration change at different steady state.

Figure 13 shows the wave velocity in the two transient processes by ±2% change of q. In the rectifying section, when q takes a negative step change, the system takes about 20 h to reach the new steady state, which is about two times more than the response time of the positive change of q. Also, the profile travels much farther from the original position. Meanwhile results in the stripping section are contrary to the rectifying section. In general, profile likely travels farther and takes longer time to stabilize when profile is driven away from the feed tray. In Figure 12, it is obvious that the sharpest points are very close to the feed tray, there is little space left for the profile to travel close to the feed tray.

Figure 14 shows the wave velocity when the profile travels away from the balanced state and then returns to the original position. The much longer time is taken for the returning process than the departing process. These asymmetric characters described by above nonlinear wave model agree with the results of ITCDIC research based on the rigorous model,[12] further revealing the validity of the proposed wave model.

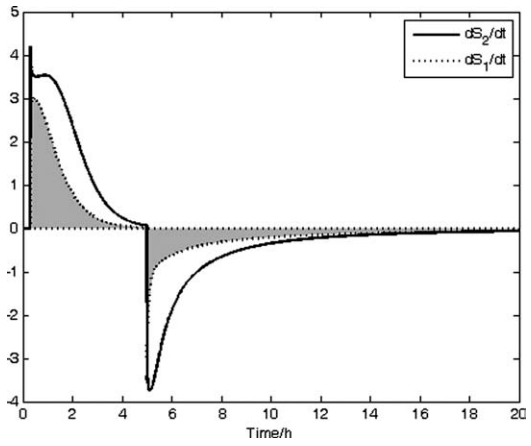

Figure 14. Wave velocity during transition departing from and back to the balanced steady state.

Inverse response

In the numerical simulation of the above proposed nonlinear wave model of ITCDIC, another interesting nonlinear phenomenon is discovered. When the feed thermal condition q is slightly changed by 0.02%, the system presents an inverse response.

As shown in Figure 15, the initial responses of $X_{r\_\max}$ and $X_{s\_\min}$ are in opposite directions to where they eventually end up. Since the feed thermal condition q has a stronger impact on the overhead product, inverse time of the stripping section is much smaller than the one of the rectifying section.

Moreover, responses of $X_{r\_\max}$ and $X_{s\_\min}$ are very similar to the product mole fraction on the two ends of ITCDIC, which reveals the efficiency of the parameters used in the profile trial functions.

Conclusions

In this work, the distinct wave traveling characteristics of ITCDIC is explored in detail based on the proposed general wave velocity with varied molar flow rates. The error of the wave position tracked by the general wave velocity and

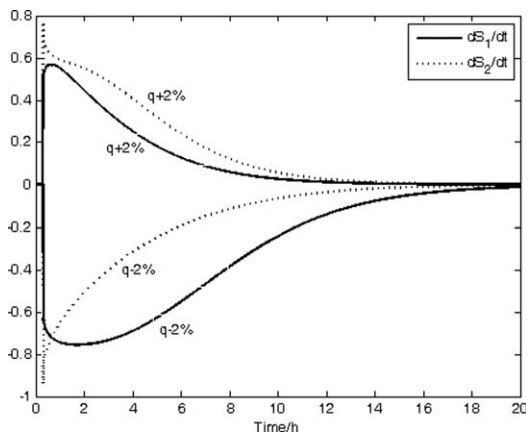

Figure 13. Wave velocity during transition caused by ±2% change of q.

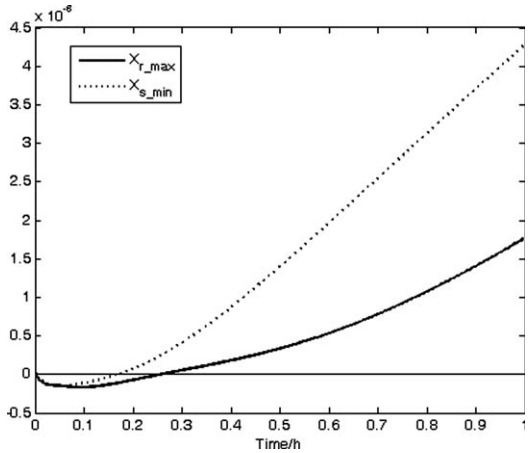

Figure 15. Response of $X_{r\_\max}$ and $X_{s\_\min}$ to 0.02% step change of q.

shock wave velocity presents the great shape influence on the movement of wave profile in ITCDIC. A further cause-effect analysis of the error is carried out based on the derived natural wave velocity, which presents a distinct wave traveling phenomenon that self-sharpening wave and nonsharpening wave co-exist in the dynamic process of ITCDIC. And further analysis reveals a fact that shape change of the self-sharpening wave in ITCDIC is much more obvious than that in CDIC. Based on the above analysis, a novel wave velocity based on the profile trial function is derived by combining the material balance relations and thermal coupling relations. A nonlinear wave model of ITCDIC is therefore established. In the illustrating application in benzene-toluene system, the component concentration prediction of the proposed wave model is compared with the first-principle model[2,12] of ITCDIC in detail, and the research results highly confirm the accuracy of the proposed nonlinear wave model. Moreover, the model is employed to explore the distinct dynamic behavior of ITCDIC like asymmetric behavior and inverse behavior. Results are in excellent agreement with the results from the first-principle model, and further prove the validity of the proposed nonlinear wave model of ITCDIC.

Acknowledgments

The authors thank the anonymous reviewer very much for his helpful suggestions for improving the manuscript. This work is supported by National Natural Science Foundation of China (Grant 50876093), International Cooperation and Exchange Project of Science and Technology Department of Zhejiang Province (Grant 2009C34008), National High Technology Research and Development Program (863, Grant 2006AA05Z226) and Zhejiang Provincial Natural Science Foundation for Distinguished Young Scientists (Grant R4100133), and their supports are thereby acknowledged.

Notation

a,b,c = coefficient of the Antoine equation
F = feed rate (kmol/h)
f = feed stage
GMC = generic model control
H = stage holdup (kmol)
h = $H/\Delta z$ (kmol/m)
IMC = internal model control
j = the stage number
k_r,k_s = characterize the tangent of the inflection points S_1 and S_2
L = liquid flow rate (kmol/h)
NMPC = nonlinear model predictive control
Pr = pressure of rectifying section (Mpa)
Ps = pressure of stripping section (Mpa)
$P_{vp,j}$ = vapor saturated pressure in stage j (Mpa)
Q = energy required (kW)
q = feed thermal condition
S_1 = inflection point of rectifying section
S_2 = inflection point of stripping section
t = time (h)
UA = heat transfer rate (kW/K)
V = vapor flow rate (kmol/h)
w_1,w_2 = the net flow of the light component to or from the column in rectifying and stripping sections respectively
X = mole fraction of liquid
$\tilde{X}$ = the liquid mole fraction in the moving wave coordinates
$\hat{X}$ = the estimation of liquid mole fraction
X_{r_min}, X_{r_max} = the asymptotic limits of the rectifying section
X_{s_min}, X_{s_max} = the asymptotic limits in the stripping section
Y = mole fraction of vapor
Z_f = mole fraction of feed
z = dimensionless spatial coordinate equals$\bar{z}/\Delta z$, and Δz is the HETP and $\bar{z}$ is spatial coordinate.

Greek letters

α = relative volatility
λ = latent heat (kJ/kmol)
ϕ_1, ϕ_2 = the influence of the shapes of the two concentration profiles in rectifying and stripping sections respectively
$\varepsilon_1 = z - S_1$
$\varepsilon_2 = z - S_2$

Subscripts

f = feed stage
j = stage number (counted from the top to the bottom, namely, from 1 to n)
r = the rectifying section
s = the stripping section

Literature Cited

1. Mah RSH, Nicholas JJ, Wodnik RB. Distillation with secondary reflux and vaporization: A comparative evaluation. *AIChE J*. 2004; 23:651–658.
2. Liu X, Qian J. Modeling control and optimization of ideal internal thermally coupled distillation columns. *Chem Eng Technol*. 2000;23: 235–241.
3. Huang K, Shan L, Zhu Q, Qian J. Design and control of an ideal heat-integrated distillation column (ideal HIDiC) system separating a close-boiling ternary mixture. *Energy*. 2007;32:2148–2156.
4. Gadalla M, Jiménez L, Olujic Z, Jansens PJ. A thermo-hydrolic approach to conceptual design of an internally hear-integrated distillation column (i-HIDiC). *Comput Chem Eng*. 2007;31:1346–1354.
5. Olujic Z, Sun L, de Rijke A, Jansens PJ. Conceptual design of an internally heat integrated propylene-propane spliter. *Energy*. 2006; 31:3083–3096.
6. Mali SV, Jana AK. A partially heat integrated reactive distillation: feasibility and analysis. *Sep Purif Technol*. 2009;70:136–139.
7. Gadalla MA. Internal heat integrated distillation columns (iHIDiCs)-New systematic design methodology. *Chem Eng Res Des*. 2009;87: 1658–1666.
8. Suphanit B. Design of internally heat-integrated distillation column (HIDiC): Uniform heat transfer area versus uniform heat distribution. *Energy*. 2010;35:1505–1514.
9. Ding F, Shi Y, Chen T. Gradient based identification algorithms for nonlinear Hammerstein ARMAX models. *Nonlinear Dyn*. 2006;45: 31–43.
10. Nakaiwa M, Huang K, Naito K, Endo A, Akiya T, Nakane T, Takamatsu T. Parameter analysis and optimization of ideal heat integrated distillation columns. *Comput Chem Eng*. 2001;25:737–744.
11. Huang K, Shan L, Zhu Q, Qian J. A totally heat-integrated distillation column (THIDiC)-the effect of feed pre-heating by distillate. *Appl Therm Eng*. 2008;28:856–864.
12. Zhu Y, Liu X. Dynamics and control of high purity heat integrated distillation columns. *Ind Eng Chem Res*. 2005;44:8806–8814.
13. Nakaiwa M, Huang K, Endo A, Ohmori T, Akiya T. Internally Heat-Integrated distillation columns: a review. *Trans IChemE*. 2003; 81:162–177.
14. Olanrewaju MJ, Al-Arfaj MA. Development and application of linear process model in estimation and control of reactive distillation. *Comput Chem Eng*. 2005;30:147–157.
15. Khowinij S, Henson MA, Belanger P, Lawrence Megan. Dynamic compartmental modeling of nitrogen purification columns. *Sep Purif Technol*. 2005;46:95–109.
16. Benallou A, Seborg DE, Mellichamp DA. Dynamic compartmental models for separation processes. *AIChE J*. 1986;32:1068–1078.
17. Epple U. *Model reduction for nonlinear systems with distributed parameters. IFAC Control of Distillation Columns and Chemical Reactors*, Bournemouth, UK, 1986:279–284.
18. Helfferich F, Klein G. *Multicomponent chromatography-theory of interference*. New York: Marcel Dekker, 1970.

19. Luyben WL. Control of distillation coulumns with sharp temperature profiles. *AIChE J*. 1971;17:713–717.
20. Luyben WL. Profile position control of distillation columns with sharp temperature profiles. *AIChE J*. 1972;18:238–240.
21. Marquardt W. Nonlinear model reduction for binary distillation. *IFAC Control of Distillation Columns and Chemical Reactors*, Bournemouth, UK, 1986:123–128.
22. Marquardt W, Amrhein M. Development of a linear distillation model from design data for process control. *Comput Chem Eng*. 1994;18(Suppl):S349–S353.
23. Marquardt W. Nichtlineare Wellenausbreitung—Ein Weg zu reduzierten dynamischen Modellen von Stofftrennprozessen. PHD thesis, VDI Reihe 8 Nr. 161, 216 pages, VDI-Verlag GmbH, Düsseldorf 1988, Germany.
24. Marquardt W. Traveling waves in Chemical process. *Int Chem Eng*. 1990;30:585–606.
25. Kienle A. Low-order dynamic models for ideal multicomponent distillation processes using nolinear wave propagation theory. *Chem Eng Sci*. 2000;55:1817–1828.
26. Hwang YL. Nonlinear wave theory for dynamics of binary distillation columns. *AIChE J*. 1991;37:705–723.
27. Hwang YL, Graham GK, Keller II GE. Experimental study of wave propagation dynamics of binary distillation columns. *AIChE J*. 1996; 42:2743–2760.
28. Hwang YL, Helfferich FG. Nonlinear waves and asymmetric dynamics of countercurrent separation processes. *AIChE J*. 1989;35: 691–693.
29. Hwang YL, Helfferich FG. Dynamics of continuous countercurrent mass-transfer processes, Part II: single-component systems with nonlinear equilibria. *Chem Eng Sci*. 1988;43:1099–1114.
30. Hwang YL, Helfferich FG. Dynamics of continuous countercurrent mass-transfer processes, Part III: multicomponent systems. *Chem Eng Sci*. 1989;44:1547–1568.
31. Hwang YL, Helfferich FG. Dynamics of continuous countercurrent mass-transfer processes, Part IV: multicomponent waves and asymmetric dynamics. *Chem Eng Sci*. 1990;45:2907–2915.
32. Balasubramhanya LS, Doyle III FJ. Nonlinear control of a high-purity distillation column using a traveling-wave model. *AIChE J*. 1997;43:703–714.
33. Balasubramhanya LS, Doyle FJ III. Low Order Modeling for Nonlinear process control. *Proceedings of the American Control Conference Seattle*, Washington, June 1995:2683–2686.
34. Han M, Park S. Control of high-purity distillation column using a nonlinear wave theory. *AIChE J*. 1993;39:787–795.
35. Han M, Park S. Startup of distillation columns using profile position control based on a nonlinear wave model. *Ind Eng Chem Res*. 1999;38:1565–1574.
36. Shin J, Seo H, Han M, Park S. A nonlinear profile observer using tray temperatures for high-purity binary distillation column control. *Chem Eng Sci*. 2000;55:807–816.
37. Zhu G, Henson MA, Megan L. Low-order dynamic modeling of cryogenic distillation columns based on nonlinear wave phenomenon. *Sep Purif Technol*. 2001;24:467–487.
38. Bian S, Henson MA. Nonlinear state estimation and model predictive control of nitrogen purification columns. *Ind Eng Chem Res*. 2005;44:153–167.
39. Bian S, Henson MA. Measurement selection for on-line estimation of nonlinear wave models for high purity distillation columns. *Chem Eng Sci*. 2006;61:3210–3222.
40. Roffel B, Betlem BHL, de Blouw RM. A comparison of the performance of profile position and composition estimators for quality control in binary distillation. *Comput Chem Eng*. 2003;27:1999–210.
41. Grüner S, Kienle A. Equilibrium theory and nonlinear waves for reactive distillation columns and chromatographic reactors. *Chem Eng Sci*. 1983;59:901–918.
42. Kim BK, Hwang H, Woo D, Han M. Design and control of a reactive distillation column Based on a nonlinear wave propagation theory: production of terephthalic acid. *Ind Eng Chem Res*. 2010;49: 4297–4307.
43. Hankins NP. A non-linear wave model with variable molar flows for dynamic behaviour and disturbance propagation in distillation columns. *Chem Eng Res Des*. 2007;85:65–73.
44. Hankins NP, Hellferich FG. On the concept and application of partial coherence in non-linear wave propagation. *Chem Eng Sci*. 1999;54:741–764.
45. Wazwaz AM. The tanh method for traveling wave solutions of nonlinear equations. *Appl Math Comput*. 2004;154:713–723.

Manuscript received Sept. 30, 2010, and revision received Mar. 29, 2011.